

# Semiconducting ZnO Nanofibers as Gas Sensors and Gas Response Improvement by SnO<sub>2</sub> Coating

Jaehyun Moon, Jin-Ah Park, Su-Jae Lee, and Taehyoung Zyung

ZnO nanofibers were electro-spun from a solution containing poly 4-vinyl phenol and Zn acetate dihydrate. The calcination process of the ZnO/PVP composite nanofibers brought forth a random network of polycrystalline würtzite ZnO nanofibers of 30 nm to 70 nm in diameter. The electrical properties of the ZnO nanofibers were governed by the grain boundaries. To investigate possible applications of the ZnO nanofibers, their CO and NO<sub>2</sub> gas sensing responses are demonstrated. In particular, the SnO<sub>2</sub>-deposited ZnO nanofibers exhibit a remarkable gas sensing response to NO<sub>2</sub> gas as low as 400 ppb. Oxide nanofibers emerge as a new proposition for oxide-based gas sensors.

**Keywords:** Nanofiber, semiconducting oxide, electrical properties, gas sensor.

## I. Introduction

The electrical properties of semiconducting oxides change upon exposure to gas. This feature has been applied toward the creation of gas sensors [1]. The gas sensing responses of oxide materials can be improved with an increase in surface-area-to-volume ratio. Therefore, the development of oxide materials with a one-dimensional geometry is highly desirable. One-dimensional oxide fibers with nanometric in-diameter dimension can be produced using an electrospinning (ES) method [2]. In ES processing, an electrical field is applied to a viscous polymeric solution, which contains an oxide forming constituent, to spun nanofibers. The ES solution is ejected from a needle in order to collect oxide/polymer composite nanofibers. Later, the composite is calcinated to obtain polycrystalline oxide nanofibers [3]-[5].

In this article, we report on ZnO nanofibers as advanced gas sensors. First, experimental topics such as an ES facility set-up and ES solution are discussed. In the next section, the structural and electrical properties of ZnO nanofibers are investigated. Finally, we evaluate the gas sensing response of ZnO nanofibers, both for reducing and oxidizing gases. We conclude this article by addressing the technical issues of the ES process which must be overcome to make ES a viable nanotechnology.

## II. Experiments

### 1. ES Facility and Process

Figure 1(a) summarizes the ES process of fabricating oxide nanofibers. The ES solution is fed by a syringe pump into a metallic needle or an orifice. ES solutions for forming oxide

---

Manuscript received Apr. 1, 2009; revised July 6, 2009; accepted July 20, 2009.

Jaehyun Moon (phone: +82 42 860 5639, email: jmoon@etri.re.kr), Jin-Ah Park (email: japak@etri.re.kr), Su-Jae Lee (email: leesujae@etri.re.kr), and Taehyoung Zyung (email: thz@etri.re.kr) are with the Convergence Components & Materials Research Laboratory, ETRI, Daejeon, Rep. of Korea.  
doi:10.4218/etrij.09.1209.0004

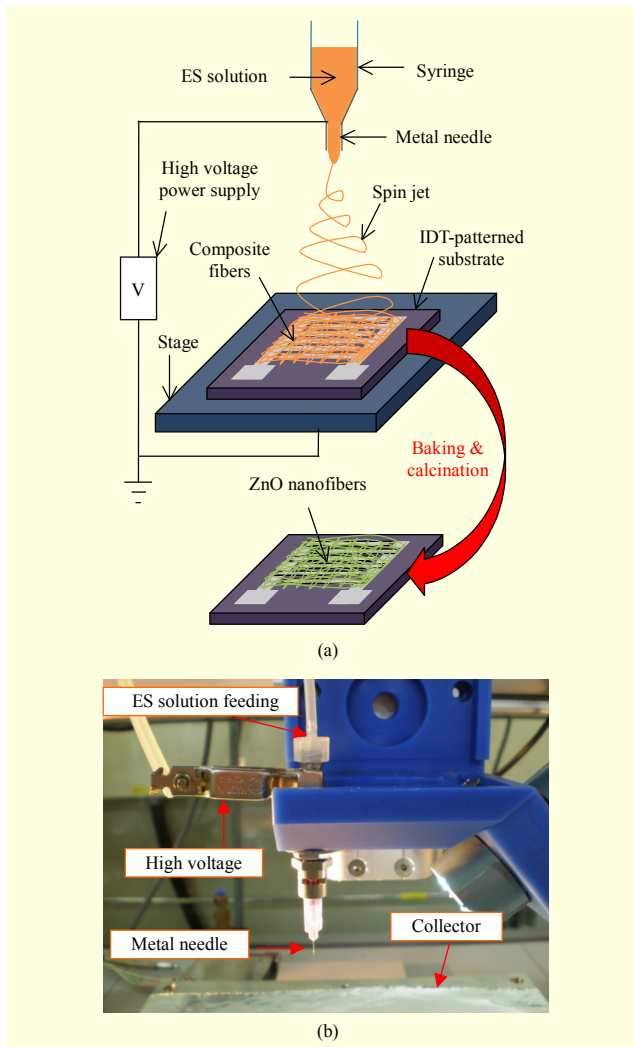


Fig. 1. (a) Schematics of the ES process and (b) a photo of an actual ES facility.

nanofibers are mainly composed of an oxide precursor and liquid polymer solutions. In the presence of an applied electrical field, the ES solution is drawn toward the collector. The collector can be either an electrical ground or a high voltage part. In practice, the applied electrical field has a magnitude of a few kilovolts. The squeezed ES solution undergoes two distinct regimes in fiber formation. In the first regime, which is usually called the Taylor cone regime, the force balance between gravity and electric polarization force tends to elongate the ES solution. The tangential electrical force acts on the surface to render the ES solution stream into a conical shape. The second regime is a rather complicated step in which various instability components contribute to disturbing the Taylor cone. Fridrikh and his fellow researchers have applied an electro-hydrodynamic (EHD) theory to model the instability of an ES solution stream [6]. Important parameters that govern the second regime are surface tension,

viscosity, electrical field, and surface charge density. Collected electro-spun nanofibers are organic/inorganic composite in nature and have a macroscopic appearance of a non-woven mat. Finally, calcinations are performed to decompose the polymeric constituents and obtain the oxide nanofibers.

Figure 1(b) captures the essential part of our ES facilities. The ES solution was loaded into a plastic syringe that has a stainless steel orifice. The orifice diameter is 650  $\mu\text{m}$  and the solution feeding rate of the solution was fixed at 0.2 ml/h. A voltage of 6 kV was applied across a distance of 5 cm between the orifice and collector.

The ZnO ES solution was prepared by mixing a ZnO acetic acid ( $\text{Zn}(\text{CH}_3\text{COO})\cdot 2\text{H}_2\text{O}$ ) containing solution, poly 4-vinyl phenol (PVP,  $M_w=20000$ ), and ethanol. The three materials were mixed at a weight ratio of 5:3:1 and stirred thoroughly for 5 hours at 60°C to obtain a homogenous solution. In the ES process, it is crucial to adjust the rheology of the ES solution. If the viscosity of the ES solution is too low, electro-spun fibers aggregate to form beads. In the opposite case, the applied electrical field cannot overcome the viscous drag force. In such a case, clogging of the orifice is observed. In our ES facility set-up, we found that a viscosity of 1,200 cps yielded the best result. The concentration of the ZnO acetic acid solution was 0.4 mol/L. PVP was added to adjust the solution viscosity, and ethanol was added to dissolve the PVP and to facilitate the solvent evaporation during the ES process. In addition, ethanol facilitates local polarization in the solution. Electrospun nanofibers were collected on  $\text{SiO}_2/\text{Si}$  (100) supports. Baking was performed at 250°C for 30 minutes to remove the solvents and form ZnO/PVP composite nanofibers. Later, the composite nanofibers were calcinated at 600°C for 90 minutes to obtain ZnO nanofibers. All heat treatments were performed in an atmospheric environment.

## 2. Structural Characterizations, Electrical Properties, and Gas Responses of ZnO Nanofibers

The morphology, composition, and crystal structure of ZnO nanofibers were investigated using scanning electron microscopy (SEM), electron dispersive spectroscopy (EDS), and X-ray diffraction (XRD) methods, respectively. To probe the phase of the nanofibers accurately, glancing angle XRD was used. The angle of the incident beam was 2°.

The electrical properties and gas sensing performance were measured and evaluated using a Pt interdigital electrode (Pt-IDEs) patterned  $\text{SiO}_2/\text{Si}$  substrate. The finger width, finger gap, and overlap length of the Pt-IDE were 15  $\mu\text{m}$ , 10  $\mu\text{m}$ , and 500  $\mu\text{m}$ , respectively.

Using an impedance/gain phase analyzer (Solatron SI 1260), impedance measurements were performed in a frequency

range from 1 MHz to 10 MHz at an AC voltage level of 500 mV. The DC current–voltage (*I*–*V*) characteristics were measured using a precision analyzer (Keithley 237).

In an effort to improve the gas sensing responses ( $R_S$ ) of the ZnO nanofibers, we used a pulsed laser deposition (PLD) method to deposit SnO<sub>2</sub> on their surfaces. A KrF excimer laser of  $\lambda=248$  nm was used to ablate the target at room temperature. The PLD process was carried out with a laser energy of 3 J/cm<sup>2</sup> and a repetition rate of 2 Hz. The oxygen pressure was 26.66 Pa. Subsequently, the SnO<sub>2</sub>-deposited ZnO nanofibers were annealed at 600°C for 30 minutes in air to crystallize SnO<sub>2</sub>. Our method must be contrasted with a conventional noble metal addition method for an improvement of the  $R_S$  of oxide gas sensors [7].

The responses of the ZnO nanofibers and SnO<sub>2</sub>-deposited ZnO nanofibers to CO and NO<sub>2</sub> gases were evaluated by measuring the resistance change upon exposure to various concentrations of the gases. A ZnO nanofiber sensor was placed in a sealed chamber equipped with a heater. The chamber was connected to a Keithley 237 device that measured the resistance and a gas flow system that controlled the gas concentration. The resistance was measured at a fixed voltage of 0.2 V. Various concentrations of gases were obtained by diluting premixed gases with air. The concentration of the premixed CO and NO<sub>2</sub> gases were 50 ppm and 20 ppm, respectively.

### III. Results and Discussion

#### 1. Structural Characterizations of ZnO Nanofibers

Figure 2 shows SEM images of ZnO/PVP composite nanofibers, ZnO nanofibers, and SnO<sub>2</sub>-deposited ZnO nanofibers. In all cases, the distributions of the nanofibers are fairly random with no distinct alignment. The surfaces of the composite fibers are smooth and their diameters are between 80 nm and 150 nm as shown in Fig. 1(a). After the calcination process, the diameters of composite nanofibers shrink significantly to diameters between 50 nm and 70 nm as shown in Fig. 2(b). The shrinkage is due to the removal of the PVP during the calcination process. The inset of Fig. 2(b) reveals that the surfaces of ZnO nanofibers consist of grains which are connected in the direction of the fiber strand. The sizes of the grains (about 50 nm) are comparable to the diameters of nanofibers. Compared to the surface morphology of ZnO nanofibers, the surface of SnO<sub>2</sub>-deposited ZnO nanofibers exhibits finer grains.

Figure 3(a) shows the XRD patterns of the ZnO/PVP composite nanofibers, ZnO nanofibers, and SnO<sub>2</sub>/ZnO composite nanofibers. The XRD pattern of ZnO/PVP

composite nanofibers shows that the pre-calcinated composite nanofibers are in an amorphous state. Calcinated nanofibers show the characteristic peaks of wurtzite ZnO. The SnO<sub>2</sub>-deposited ZnO nanofibers show an extra peak around  $2\theta = 40^\circ$ , which is indexed as the (200) of rutile SnO<sub>2</sub>. Therefore, we conclude that the deposited SnO<sub>2</sub> has crystallized on the surfaces of the ZnO nanofibers. As the XRD results indicate, no crystallographic preference is observed but a random polycrystalline structure. Considering the broad full-width half maxima of the main XRD peaks of ZnO nanofibers and SnO<sub>2</sub>-deposited ZnO composite nanofibers, the crystallites are thought to have high defect densities. In such a case, the surface packings can be different from those of defect free crystallites, and the surface free energies are not necessarily inversely proportional to the atomic packing of the

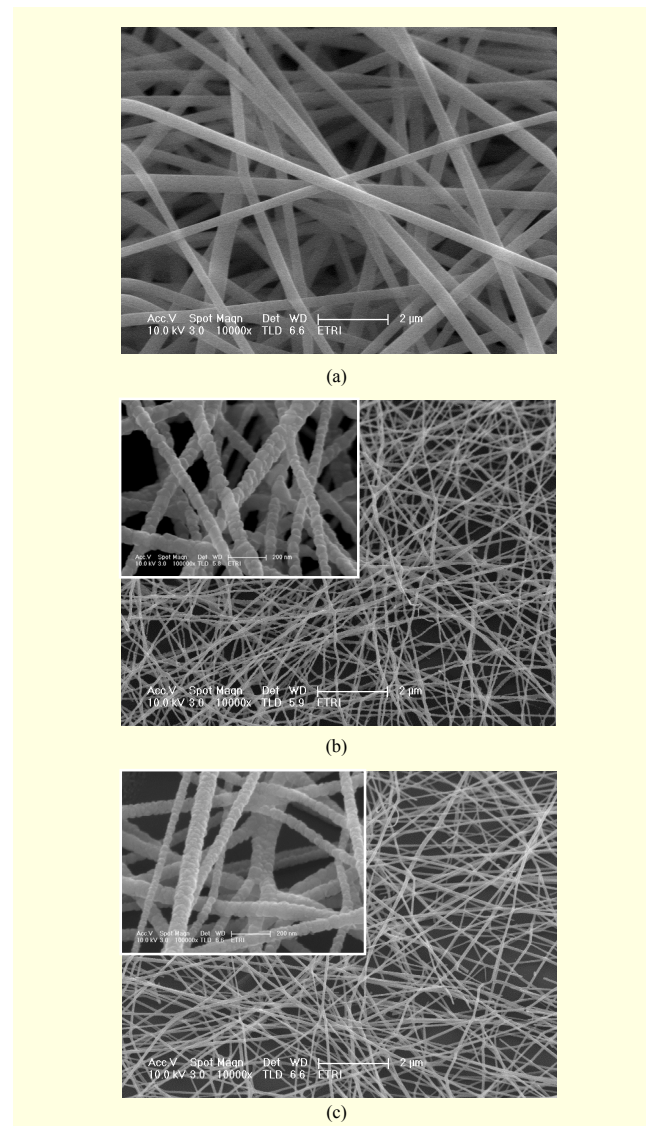
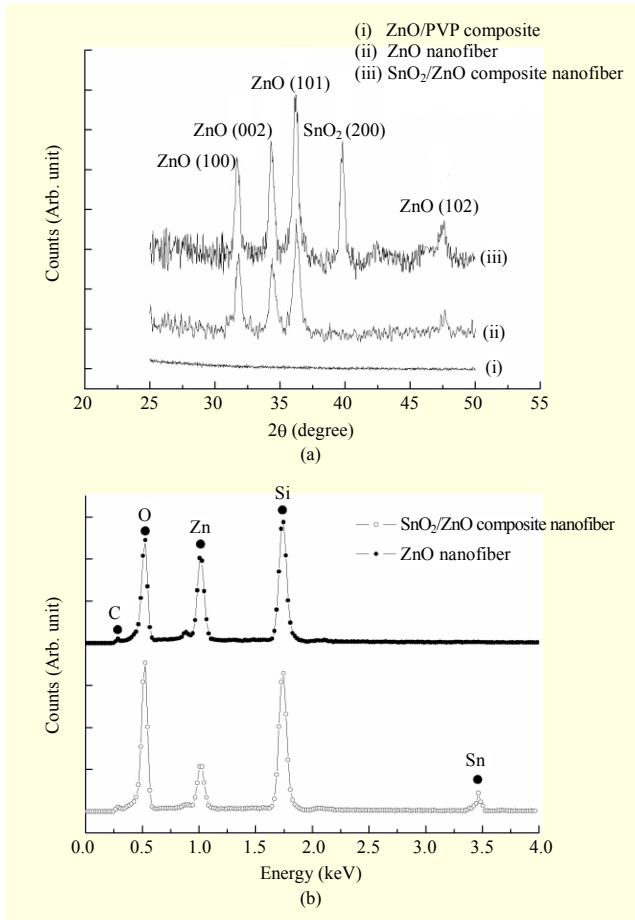


Fig. 2. SEM images of (a) ZnO/PVP composite nanofibers, (b) ZnO nanofibers, and (c) SnO<sub>2</sub>-deposited ZnO nanofibers.



**Fig. 3.** (a) XRD patterns of ZnO/PVP composite nanofibers, ZnO nanofibers, and SnO<sub>2</sub>/ZnO composite nanofibers and (b) EDS spectra of ZnO nanofibers and SnO<sub>2</sub>/ZnO composite nanofibers.

crystallographic planes, leading to a random polycrystalline structure. Figure 3(b) shows the composition of the ZnO nanofibers and SnO<sub>2</sub>-deposited ZnO nanofibers. The Si peak originates from the substrate; therefore, it is irrelevant to the composition of the nanofibers. The concentration of carbon is very low, indicating that our calcination condition is sufficient to decompose all organic materials. These results demonstrate the feasibility of producing ZnO nanofibers and SnO<sub>2</sub>-deposited ZnO nanofibers with the current facility set-up and ES solution.

## 2. Electrical Properties of ZnO Nanofibers

ZnO nanofibers can be considered as having two resistive components, one for the grain interiors and another for the grain boundaries (GBs). Therefore, we expect to observe two semicircles in a Cole-Cole plot. Based on this idea, we may construct an equivalent circuit diagram as in the inset of Fig. 4(a). However, only one semicircle is obtained from the

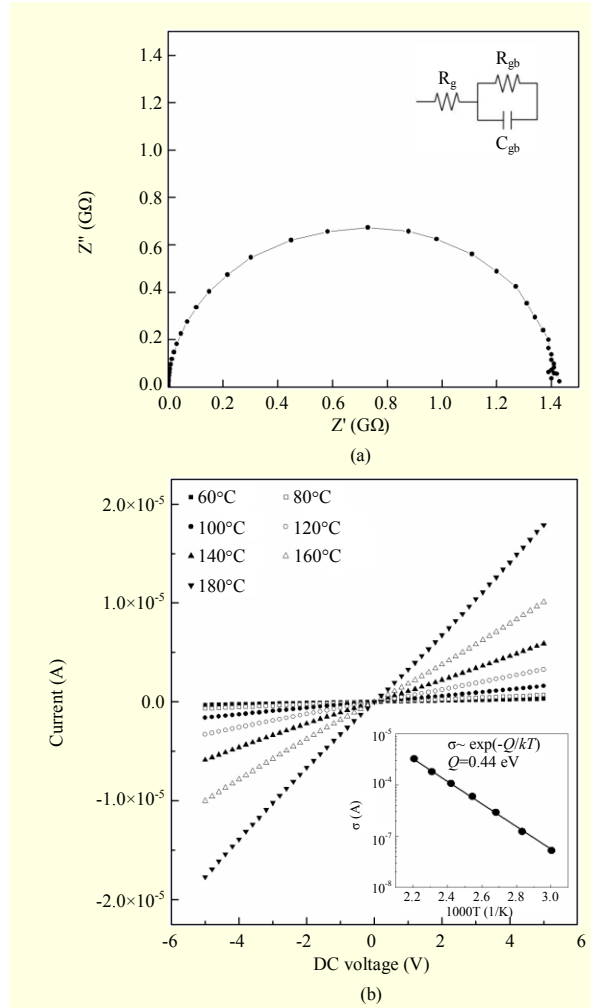


**Fig. 4.** (a) Cole-Cole plot of ZnO nanofibers and (b) the DC conductivities of ZnO nanofibers as a function of temperature.

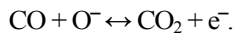
measurement in Fig. 4(a), which indicates that one component dominates the electrical properties. Studies on single crystal semiconducting oxides suggest a resistivity of approximately  $10^{-3} \Omega\text{-m}$  [8]. Referring to the results in Fig. 4(a), such values are too small to be effectively appreciable. Figure 4(b) shows the DC I-V relationship as a function of temperature. Ohmic behaviors are observed in a voltage range from -5 V to 5 V.

Also, conductivity increases with an increase in temperature; thus, electrical conduction is thermally assisted. Based on this observation, we constructed an Arrhenius plot, as shown in the inset of Fig. 4(b), to obtain the activation energy ( $Q$ ). A  $Q$  of about 0.44 eV was extracted from a relation of  $\sigma \propto \exp(-Q/kT)$ , where  $k$  and  $T$  are the Boltzmann constant ( $=8.62 \times 10^{-5} \text{ eV/K}$ ) and absolute temperature, respectively. Our activation energy is comparable to the values obtained in studies on GBs of polycrystalline semiconducting metal oxides [9]. These support that the electrical properties of ZnO nanofibers are governed by

the GBs. The activation energy can be interpreted as the height of the double Schottky barrier, which originates from the acceptor states of GBs. Due to the change in the height of the double Schottky barrier upon exposure to gases, semiconducting oxides can be applied as gas sensors [10]. Because of the high ratio of surface area to volume, nanofibers are attractive for gas sensors.

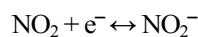
### 3. Gas Responses of ZnO Nanofibers

Figure 5(a) shows the gas sensing responses of ZnO nanofibers to CO. In the CO concentration range considered in this work, the resistance of the ZnO nanofibers decreases upon exposure to CO. Exposure to higher CO concentration leads to a larger resistance drop. Full recovery to the initial resistance of the ZnO nanofibers was not achieved in the interval time of 120 seconds. Residual CO can be one explanation for this. The surface reaction involved in CO detection may be written as



As can be noticed, one extra electron ( $\text{e}^-$ ) is released per reaction. Released electrons contribute to lowering the Schottky barrier and narrowing the width of the depleted layer, which leads to a decrease in the resistance of ZnO nanofibers.

In contrast, the resistance of the  $\text{SnO}_2$ -deposited ZnO nanofibers increases upon exposure to  $\text{NO}_2$  (Fig. 5(b)). Notably, the  $\text{SnO}_2$ -deposited ZnO composite nanofibers show a response to  $\text{NO}_2$  concentrations as low as 400 ppb. Compared to oxide gas sensors that use an identical material combination, our sensors exhibit a far better response and detection limit [11]. Relevant reactions taking places at the surfaces of nanofibers may be written as



In the case of  $\text{NO}_2$ , the opposite phenomenon occurs, which leads to an increase in resistance. A huge difference in the response is observed between CO and  $\text{NO}_2$  gas sensing. The response of  $\text{SnO}_2$ -deposited ZnO nanofibers to  $\text{NO}_2$  is 100 at a concentration of 5.5 ppm, while a response of 2.3 is obtained for ZnO nanofibers to CO of 25 ppm. Recalling the two-phase nature of  $\text{SnO}_2$ -deposited ZnO nanofibers, it is thought that the improvement in response by  $\text{SnO}_2$  deposition is due to the increase in numbers of  $\text{NO}_2$  adsorption sites. Thus, the change in resistance upon gas exposure becomes more sensitive. Conventionally, responses of oxide gas sensors have been enhanced by the addition of noble metals such as Ag, Pt, and Pd. These noble metals are known to increase the rate of surface reaction at the surface due to catalytic actions [7]. In contrast, our method for improving the response relies on providing an additive that directly changes the resistance.

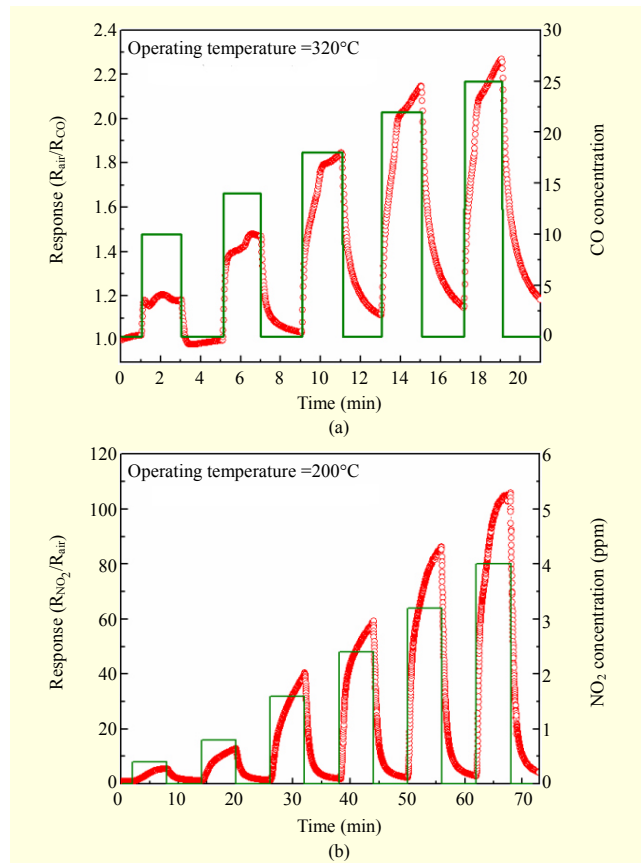


Fig. 5. (a) Responses of the ZnO nanofibers-based chemosensor to CO and (b) responses of the  $\text{SnO}_2/\text{ZnO}$  composite nanofiber-based chemosensor to  $\text{NO}_2$ .

Some closing comments regarding the ES technology are worthwhile here. The ES process for oxide nanofibers is still in the developmental stage and many application areas remain unexplored [12]-[14]. There are some problems yet to be solved. First of all, in order to control and predict the morphologies and electrical properties in a comprehensive manner, the development of ES solutions must be pursued, even though many oxide ES solutions are available. Second, in order to expand the application of nanofibers into the category of electrical devices, facilities and processes must be designed in a way that allows alignment and location of nanofibers. Finally, presumably due to the calcination process, the productivity of the ES process for fabricating oxide nanofibers is still low. Therefore, improvement in the fiber collection process is needed.

### IV. Summary

In summary, this study presents an ES processing method for producing ZnO nanofibers from a solution containing PVP and Zn acetic acid. Calcination of ZnO/PVP composite nanofibers

brought forth ZnO nanofibers from 30 nm to 70 nm in diameter with a polycrystalline wurtzite structure. Also, SnO<sub>2</sub>-deposited ZnO composite nanofibers were produced to improve the gas sensing response. The CO and NO<sub>2</sub> gas sensing responses of ZnO nanofibers were demonstrated. SnO<sub>2</sub>-deposited ZnO composite nanofibers showed an exceptionally high capability in detecting NO<sub>2</sub> gas concentrations as low as 400 ppb. ZnO oxide nanofiber-based gas sensors demonstrate great potential for the rapid development of advanced portable gas monitors.

## Acknowledgement

The authors wish to acknowledge the support of the Electronics and Telecommunications Research Institute, Korea.

## References

- [1] N. Yamazoe, G. Sakai, and K. Shimanoe, "Oxide Semiconductor Gas Sensors," *Catalysis Sur. Asia*, vol. 7, 2003, pp. 63-75.
- [2] R. Ramaseshan et al., "Nanostructured Ceramics by Electrospinning," *J. Appl. Phys.*, vol. 102, 2007, pp. 111101-111117.
- [3] Q. Wan et al., "Fabrication and Ethanol Sensing Characteristics of ZnO Nanowire Gas Sensors," *Appl. Phys. Lett.*, vol. 84, 2004, pp. 3654-3656.
- [4] Y. Wang et al., "Synthesis and Characterization of Tin Oxide Microfibres Electrospun from a Simple Precursor Solution," *Semicond. Sci. Technol.*, vol. 19, 2004, pp. 1057-1060.
- [5] J. Moon et al., "Structure and Electrical Properties of Electrospun ZnO-NiO Mixed Oxide Nanofibers," *Current Appl. Phys.*, vol. 9, 2009, pp. s213-s216.
- [6] S. Fridrikh et al., "Controlling the Fiber Diameter During Electrospinning," *Phys. Rev. Lett.*, vol. 90, 2003, pp. 144502-144505.
- [7] S. Matsushima et al., "Electronic Interaction Between Metal Additives and Tin Dioxide in Tin Dioxide-Based Gas Sensors," *Jpn. J. Appl. Phys.*, vol. 27, 1988, pp. 1798-1802.
- [8] S. Kim and J. Maier, "Electrical Properties of ZnO, Nanocrystalline vs. Microcrystalline Ceramics," *Electrochem. Solid-State Lett.*, vol. 6, 2003, pp. J7-J9.
- [9] J. Lee et al., "Impedance Spectroscopy of Grain Boundaries in Nanophase ZnO," *J. Mat. Res.*, vol. 10, 1995, pp. 2295-2300.
- [10] G. Korotcenkov, "Metal Oxides for Solid-State Gas Sensors: What Determines Our Choice?" *Mat. Sci. Eng. B*, vol. 139, 2007, pp. 1-23.
- [11] C. Liangyuan et al., "Synthesis of ZnO-SnO<sub>2</sub> Nanocomposites by Microemulsion and Sensing Properties for NO<sub>2</sub>," *Sens. Act. B*, vol. 134, 2008, pp. 360-366.
- [12] A. Greiner and J.H. Wendorff, "Functional Self-Assembled Nanofibers by Electrospinning," *Adv. Polymer Sci.*, vol. 219,

2008, pp. 107-171.

- [13] D. Li and Y. Xia, "Electrospinning of Nanofibers: Reinventing the Wheel?" *Adv. Mat.*, vol. 16, 2004, pp. 1151-1170.
- [14] H.Y. Yu et al., "Nanogap Array Fabrication Using Doubly Clamped Freestanding Silicon Nanowires and Angle Evaporations," *ETRI J.*, vol. 31, no. 4, Aug. 2009, pp. 351-356.



**Jaehyun Moon** received his BS degree from Korea University, Seoul, Rep. of Korea, in 1995, and his PhD in materials science and engineering from Carnegie Mellon University, Pittsburgh, USA, in 2003. From 2003 to 2004, he was a post-doctoral associate at Max-Planck Institute, Stuttgart, Germany. He joined ETRI in 2004. His current research interests include flexible display, low temperature Si processes, nanofibers, and interface studies of materials.



**Jin-Ah Park** received the BS degree from Gyeongsang National University, Jinju, Rep. of Korea, in 1998, and the PhD in electrical engineering from Dongguk University, Busan, Rep. of Korea, in 2006. As a post-doctoral associate, he joined ETRI in 2007. His current research interests include oxide electronics as well as nanomaterials and their applications.



**Su-Jae Lee** received the BS degree in physics from Kyungshung University, Korea, in 1986 and the MS and PhD degrees in physics from Pusan National University, Busan, Korea, in 1988 and 1997, respectively. Since he joined ETRI in 1997, he has been involved in the development of microwave tunable dielectric thin films and tunable devices for next-generation wireless communication and development of dielectric gate materials of poly-Si TFT on a plastic substrate for flexible display. His research interests include the development of new multifunctional nanostructured oxides for the creation of next-generation nano-oxide electronics devices and chemical gas sensors.



**Taehyung Zyung** graduated Seoul National University in 1977 and worked at KIST as a researcher for 3 and half years from 1978. He received the PhD in physical chemistry from Texas Tech University in 1986. He performed post-doctoral study as a research associate at the University of Illinois at Urbana-Champaign from 1986 to 1989. He joined ETRI in 1989 and has worked on organic semiconductor devices. He has published articles in about 100 SCI journals and has filed about 30 patents.